

ARTICLE

Magnetic Solid-Phase Extraction of Phthalate Esters from Environmental Water Samples using Fibrous Phenyl-functionalized $\text{Fe}_3\text{O}_4@\text{SiO}_2@\text{KCC}-1$

Xue-zheng Zhou^a, Xiang-yang Yan^b, Ling Zhu^a, Ming Ma^a, Ya Dai^a, Chang-guo Wang^a,
Li-jun Zhu^{a*}, Ke-jie Yu^b, Shao-min Liu^{b*}

a. Chongqing Key Laboratory of Scientific Utilization of Tobacco Resources, Chongqing 400060, China

b. Department of Chemistry, University of Science and Technology of China, Hefei 230026, China

(Dated: Received on September 3, 2019; Accepted on February 26, 2020)

A new kind of phenyl-functionalized magnetic fibrous mesoporous silica ($\text{Fe}_3\text{O}_4@\text{SiO}_2@\text{KCC}-1\text{-phenyl}$) was prepared by copolymerization as an efficient adsorbent for the magnetic extraction of phthalate esters from environmental water samples. The obtained $\text{Fe}_3\text{O}_4@\text{SiO}_2@\text{KCC}-1\text{-phenyl}$ showed monodisperse fibrous spherical morphology, fairly strong magnetic response (29 emu/g), and an abundant π -electron system, which allowed rapid isolation of the $\text{Fe}_3\text{O}_4@\text{SiO}_2@\text{KCC}-1\text{-phenyl}$ from solutions upon applying an appropriate magnetic field. Several variables that affect the extraction efficiency of the analytes, including the type of the elution solvent, amount of adsorbent, extraction time and reusability, were investigated and optimized. Under optimum conditions, the $\text{Fe}_3\text{O}_4@\text{SiO}_2@\text{KCC}-1\text{-phenyl}$ was used for the extraction of four phthalate esters from environmental water samples followed by high-performance liquid chromatographic analysis. Validation experiments indicated that the developed method presented good linearity (0.1–20 ng/mL), low limit of detection (7.5–29 $\mu\text{g/L}$, $S/N=3$). The proposed method was applied to the determination of phthalate esters in different real water samples, with relative recoveries of 93%–103.4% and relative standard deviation of 0.8%–8.3%.

Key words: Fibrous mesoporous silica, Phenyl-functionalized, Magnetic solid-phase extraction, High performance liquid chromatography, Phthalate esters, Environmental water

I. INTRODUCTION

Phthalate acid esters (PAEs) are synthetic organic compounds with a large production volume and wide application in the world economy, and are a global environmental pollutant that is widely present in air, water, soil and organisms [1, 2]. These compounds are closely related to our daily life and can enter the human body through drinking water, eating, cosmetics and breathing, causing different degrees of harm to human health. Phthalates in environmental water bodies mainly come from two sources, namely, industrial wastewater and the slow release of phthalate acid esters from the solid waste accumulation, with the concentration of both sources generally being on the order of nanograms. Due to the large volume of environmental water samples and the low concentration of phthalate acid esters pollutants, a long time is required for sample pretreatment in the determination process. Up to now, various pretreatment techniques have been attempted to extract phthalate acid esters from differ-

ent samples, such as liquid-liquid extraction [3, 4], solid phase extraction [5–7], solid phase microextraction [8, 9]. Liquid-liquid extraction requires solvent consumption with high pollution and cost. solid phase extraction takes a long time, while solid phase microextraction can be performed with few kinds of extraction heads. These defects make the above methods unsuitable for rapid and efficient enrichment, separation and determination of phthalates in environmental water samples. Therefore, the development of a rapid and effective method for the separation, enrichment and determination of phthalates has attracted wide attention.

Magnetic solid phase extraction (MSPE) is a sample pretreatment method that can be used for rapid treatment of samples with large volume without column filling, uses diversified materials and shows simple operation, easy separation of magnetic materials from the matrix, and high concentration efficiency. The enrichment and separation of phthalates in environmental water bodies using magnetic solid phase extraction has also been reported [10–13]. In particular, magnetic core-shell mesoporous silica materials are favoured due to their unique advantages and are widely used for the separation and enrichment of various environmental pollutants [14–16]. The Fe_3O_4 core of magnetic core-shell mesoporous silicon has a unique magnetic respon-

*Authors to whom correspondence should be addressed. E-mail: liusm@ustc.edu.cn, zhulj@cncqti.com

se, and only one external magnetic field is needed to achieve the separation of adsorbent material and impurity matrix. At the same time, this silica shell of materials has excellent properties, such as large specific surface area, good thermal and mechanical stability, uniform pore distribution, and high adsorption capacity [17–21]. Si–OH can be condensed with organic trialkoxy silane coupling agent to obtain alkyl [22], amino [23, 24], mercapto [25], aromatic ring [26, 27], and other organic functional-group-functionalized silica materials. The introduction of organic functional groups increases the effective action sites of magnetic silica materials in practical applications, making them more targeted for the adsorption of inorganic metals and other pollutants. At the same time, the hydrophilic and hydrophobic properties of silica are also changed, making the adsorption of organic pollutants more effective [28–32].

There are three main methods for the functionalization of magnetic core-shell mesoporous silicon: (i) grafting method, that is, after magnetic mesoporous silicon is prepared, it is hydrolysed and condensed with an organosilane coupling agent, and the organic functional groups are grafted onto the material surface [33, 34]; (ii) copolycondensation, carried out mainly for the *n*-silicate ethyl ester and organosilane coupling agent mixture in the reaction of simultaneous hydrolysis condensation to obtain functional magnetic mesoporous materials [35]; (iii) the skeleton hybrid method: in the skeleton method, $(\text{EtO})_3\text{Si-R-Si}(\text{OEt})_3$ is used as a single silicon source for hydrolysis and condensation to form a material containing organic functional groups and ordered arrangement of silicon [36]. Among the three methods, the grafting method is likely to cause pore channel blockage, and the obtained distribution of functional groups is not uniform. Although the distribution of functional groups is uniform in the framework hybrid method, the silicon source precursor is very rare, meaning that it is generally necessary to conduct pre-synthesis, and the method is tedious. Copolycondensation does not easily cause the blockage of pore channels, and the functional groups can also be relatively uniform. The silicon source precursors can be easily obtained. Thus, copolycondensation is an effective and commonly used method of functionalization of functional groups of silicon materials.

In a previous work, we successfully synthesized a monodisperse fibrous magnetic core-shell mesoporous material $\text{Fe}_3\text{O}_4@\text{SiO}_2@\text{KCC-1}$ [37]. However, in the practical application of this material in the separation and enrichment of environmentally hazardous substances, it was found that the material lacks active sites, is too strongly hydrophilic and too weakly hydrophobic, and has a poor enrichment effect on organic pollutants. Therefore, the development of a functional modification fibrous magnetic core-shell mesoporous silicon material is still a challenging. For this purpose, based on the previous research results obtained by our research group,

in the present work, we carried out a phenyl functional modification experiment on the fibrous magnetic core-shell mesoporous silicon material, that is, a step copolycondensation method was adopted to synthesize the fibrous magnetic core-shell mesoporous silicon containing phenyl in the radial pore channels ($\text{Fe}_3\text{O}_4@\text{SiO}_2@\text{KCC-1-phenyl}$). The effect of the ratio of phenyltriethoxysilane and ethyl orthosilicate on the final morphology was investigated. The morphology and properties of the material were characterized by XRD, SQUID, TEM and N_2 adsorption/desorption, and the $\text{Fe}_3\text{O}_4@\text{SiO}_2@\text{KCC-1-phenyl}$ was applied as a magnetic solid-phase adsorbent to the enrichment and separation of phthalate acid esters in environmental water samples for the first time. The magnetic solid-phase extraction procedure was investigated systematically. Coupling this novel magnetic molecularly imprinted solid-phase extraction technique with HPLC, a feasible phenyl-functionalized $\text{Fe}_3\text{O}_4@\text{SiO}_2@\text{KCC-1-SPE-HPLC}$ (MMIP-SPE-HPLC) analytical method was established and was applied to the analysis of real samples.

II. EXPERIMENTS

A. Reagents and materials

Hexadecylpyridinium bromide (CPB, purity > 96%) and phenyltriethoxysilane (PTES, purity > 98%) were purchased from Aladdin Reagent Co., Ltd., China. Ammonium hydroxide (28%) and ethyl silicate (TEOS, 99%) of analytical grade were purchased from Sinopharm Shanghai Chemical Corp., China. The standards of four phthalate esters, including butyl benzyl phthalate (BBP), dibutyl phthalate (DnBP), diethylhexyl phthalate (DEHP), and dioctyl phthalate (DnOP) were of HPLC-grade and were purchased from Aladdin Reagent Corp., China. The HPLC-grade methanol and acetonitrile were purchased from the Tedia Company, Inc., USA. Other chemical reagents were of chemical grade.

B. Instrumentation

Morphologies and structures of materials were observed using an XL30 scanning electron microscope (Philips, Holland) and a JEM-2011 transmission electron microscope (JEOL, Japan) operating at 20 and 200 kV, respectively. The magnetisation curves of materials were examined using a SQUID magnetic susceptometer (VSM, USA) operated at 300 K. The XRD pattern was obtained with a Philips X'Pert PRO SUPER diffractometer (Philips, Holland) using nickel-filtered $\text{Cu-K}\alpha$ radiation (40 kV and 25 mA). The specific surface areas were measured by a TristarII3020 surface area analyser (Micromeritics Instrument Co., USA).

High-performance liquid chromatography (HPLC)

was performed using a Shimadzu LC-20A with an ultraviolet detector (SPD-M20A) and a GL-C18 column (250 mm \times 4.6 mm, 5 μ m) at 30 $^{\circ}$ C. The mobile phase consisted of water and methanol, and phthalate esters were separated using the following gradient elution program: 75% methanol for 5 min followed by a linear increase to 100% methanol over a 16 min period, then held for 7 min, and finally returned to 75% methanol in 7 min. The flow rate of the mobile phase was set at 0.8 mL/min. The injection volume was 20 μ L. The detection wavelength was 280 nm.

C. Synthesis of $\text{Fe}_3\text{O}_4@\text{SiO}_2@\text{KCC-1-phenyl}$

$\text{Fe}_3\text{O}_4@\text{SiO}_2$ was synthesized by the hydrothermal method [33]. Fe_3O_4 (0.5 g) was dispersed homogeneously in a mixture of ethanol (150 mL), distilled water (25 mL) and ammonium hydroxide (28 wt%, 5 mL). The mixture was mechanically stirred for 30 min. Then, TEOS (1 mL) was slowly added to the mixture under constant stirring. After stirring at 50 $^{\circ}$ C for 6 h, the $\text{Fe}_3\text{O}_4@\text{SiO}_2$ nanospheres were separated by an NdFeB magnet and was washed alternately three times with ethanol and water.

CPB (0.5 g) was dispersed utterly to *n*-pentanol (0.75 mL) and cyclohexane (15 mL) to form solution A. Dried $\text{Fe}_3\text{O}_4@\text{SiO}_2$ (0.25 g) was added to an aqueous solution (15 mL) containing urea (0.3 g) to form solution B. Solution B was added to solution A under stirring at 25 $^{\circ}$ C. Then, TEOS (1.25 mL) and PTES (0.075 mL) were added to the above solution and stirred for 10 min, after which the mixture was transferred to a 50 mL Teflon-lined autoclave and heated at 120 $^{\circ}$ C for 4 h. The obtained materials were separated by an NdFeB magnet and washed with ethanol in a Soxhlet apparatus to remove the CPB and non-polymerized residue. The resultant $\text{Fe}_3\text{O}_4@\text{SiO}_2@\text{KCC-1-phenyl}$ were washed with ethanol and dried.

D. Magnetic solid phase extraction procedure

For the magnetic solid phase extraction procedure, $\text{Fe}_3\text{O}_4@\text{SiO}_2@\text{KCC-1-phenyl}$ (20 mg) was added to the water sample (500 mL), the mixture was shaken for 10 min, the materials were then isolated from the suspension by placing an NdFeB magnet at the bottom of the vessel, and then the $\text{Fe}_3\text{O}_4@\text{SiO}_2@\text{KCC-1-phenyl}$ was washed by methanol (1.0 mL) to desorb the phthalate acid esters. The desorbed solution was filtered through a 0.45- μ m filter and then injected into the HPLC for analysis.

E. Recyclability of $\text{Fe}_3\text{O}_4@\text{SiO}_2@\text{KCC-1-phenyl}$

To investigate the recyclability of the adsorbent, the $\text{Fe}_3\text{O}_4@\text{SiO}_2@\text{KCC-1-phenyl}$ were reused for magnetic solid phase extraction. The materials were washed al-

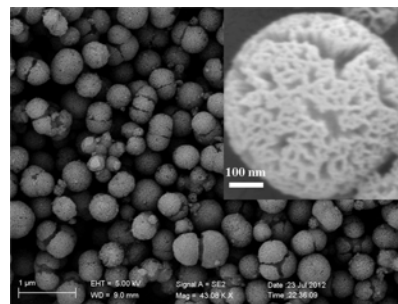


FIG. 1 The SEM images of $\text{Fe}_3\text{O}_4@\text{SiO}_2@\text{KCC-1-phenyl}$.

ternately with water and methanol several times after each magnetic solid phase extraction procedure and were dried at 100 $^{\circ}$ C.

F. Sample preparation

Three kinds of environmental water samples, including lake, river, and tap water, were collected randomly into the glass bottle to evaluate the phthalate acid esters contents in real samples. The water samples were filtered through a 0.45 μ m filter and stored in the dark. All of the water samples should be determined in 24 h to avoid the formation and interference of microorganisms.

III. RESULTS AND DISCUSSION

A. Characterization of $\text{Fe}_3\text{O}_4@\text{SiO}_2@\text{KCC-1-phenyl}$

The scanning electron microscopy (SEM) image (FIG. 1) of $\text{Fe}_3\text{O}_4@\text{SiO}_2@\text{KCC-1-phenyl}$ showed that the new adsorbent has fibrous morphology, clearly visible pore channels and good dispersity. Compared with our previously investigated material ($\text{Fe}_3\text{O}_4@\text{SiO}_2@\text{KCC-1}$) [37], this adsorbent had larger pores and looser appearance due to the addition of PTES. However, the formation of the morphology of the new adsorbent was affected by the new silicon source because phenyl side of the silicon source could no longer be coupled. Therefore, the morphology of the new material is slightly less regular than that of the previously reported material. FIG. 2 shows the representative TEM images of $\text{Fe}_3\text{O}_4@\text{SiO}_2@\text{KCC-1-phenyl}$ with different amounts of PTES. When the other conditions remained constant during the synthesis, an increase in the amount of PTES decreased the density of the fibrous layer. For the PTES content of 0.025 mL, the morphology of the $\text{Fe}_3\text{O}_4@\text{SiO}_2@\text{KCC-1-phenyl}$ could be well-maintained, and the distribution of the fibrous layer was uniform (FIG. 2(a)). With the increase in the PTES content, the fibrous layer became very sparse and the morphology was disturbed. The pore structure of the adsorbent collapsed, and no fibrous morphology or radial pores could be formed when the PTES content reached its limit value.

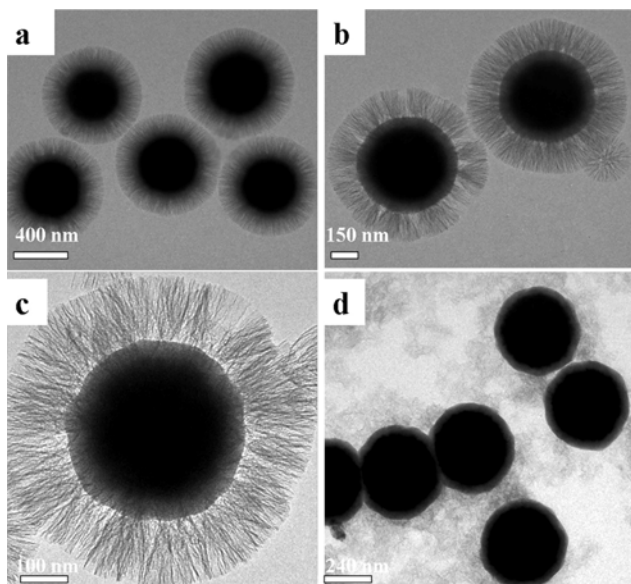


FIG. 2 The TEM image of $\text{Fe}_3\text{O}_4@\text{SiO}_2@\text{KCC-1-phenyl}$ with different content PTES of (a) 0.025 mL, (b) 0.05 mL, (c) 0.075 mL, (d) 0.1 mL $\text{Fe}_3\text{O}_4@\text{SiO}_2$, and $\text{Fe}_3\text{O}_4@\text{SiO}_2@\text{KCC-1-phenyl}$ sample.

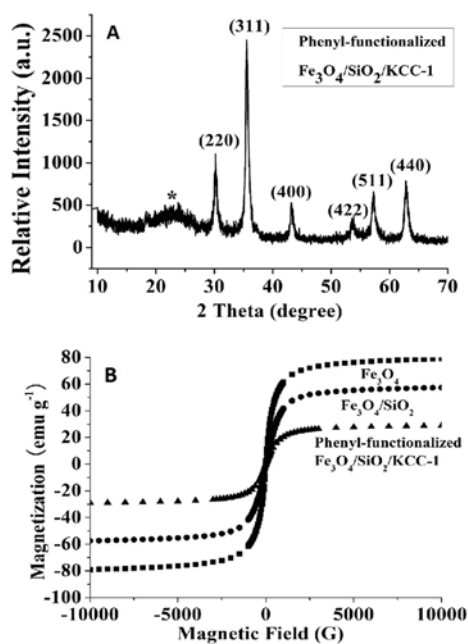


FIG. 3 (A) The wide-angle XRD pattern of $\text{Fe}_3\text{O}_4@\text{SiO}_2@\text{KCC-1-phenyl}$ and (B) magnetisation curves of the Fe_3O_4 , $\text{Fe}_3\text{O}_4@\text{SiO}_2$, and $\text{Fe}_3\text{O}_4@\text{SiO}_2@\text{KCC-1-phenyl}$ sample.

The wide-angle XRD pattern of phenyl-functionalized $\text{Fe}_3\text{O}_4@\text{SiO}_2@\text{KCC-1}$ (FIG. 3(A)) showed peaks similar to those of Fe_3O_4 (JCPDS No.19-0629), confirming that the Fe_3O_4 nanoparticles were synthesized successfully. The broad band at $2\theta=22^\circ$ was attributed to the amorphous mesoporous silica

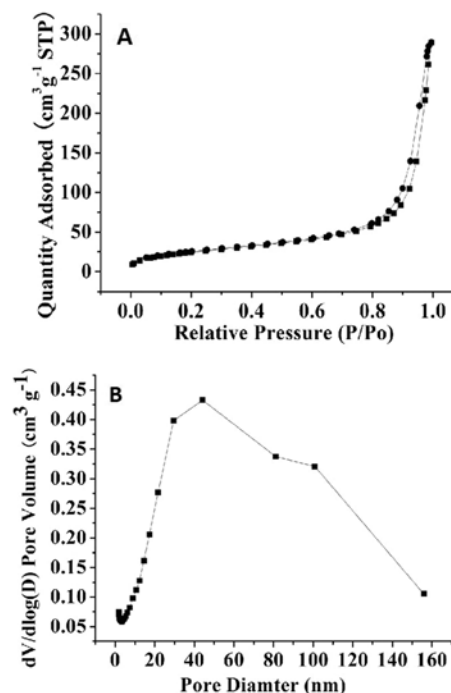


FIG. 4 (A) The N_2 adsorption-desorption isotherm of $\text{Fe}_3\text{O}_4@\text{SiO}_2@\text{KCC-1-phenyl}$ and (B) the pore size distribution curve of $\text{Fe}_3\text{O}_4@\text{SiO}_2@\text{KCC-1-phenyl}$.

(JCPDS No.29-0085). As shown in FIG. 3(B), the saturation magnetizations of Fe_3O_4 , $\text{Fe}_3\text{O}_4@\text{SiO}_2$, and phenyl-functionalized $\text{Fe}_3\text{O}_4@\text{SiO}_2@\text{KCC-1}$ samples were 79, 57 and 29 emu/g, respectively. No hysteresis, remanence, and coercivity was observed. These data showed that the nanoparticles still had good magnetism that could satisfy the requirement of magnetic solid phase extraction absorbents.

The N_2 adsorption-desorption isotherm of $\text{Fe}_3\text{O}_4@\text{SiO}_2@\text{KCC-1-phenyl}$ (FIG. 4(A)) shows typical type IV isotherms, and the BET surface and pore volume were $92.54 \text{ m}^2/\text{g}$ and $0.44 \text{ cm}^3/\text{g}$, respectively. The pore size distribution curve of $\text{Fe}_3\text{O}_4@\text{SiO}_2@\text{KCC-1-phenyl}$ (FIG. 4(B)) shows that the pore size of the nanoparticles was distributed mainly between 30 and 45 nm. The results indicated that an increase in the pore size of the nanoparticles decreased the BET surface area due to the modification of phenyl which interfered with the formation of the morphology of the nanoparticles, and the same conclusion was reached based on the TEM results.

B. Optimization of magnetic solid phase extraction conditions

1. Amount of $\text{Fe}_3\text{O}_4@\text{SiO}_2@\text{KCC-1-phenyl}$ absorbents

The amount of $\text{Fe}_3\text{O}_4@\text{SiO}_2@\text{KCC-1-phenyl}$ was investigated for the improvement of the adsorption efficiency. As shown in FIG. 5(A), only a small amount

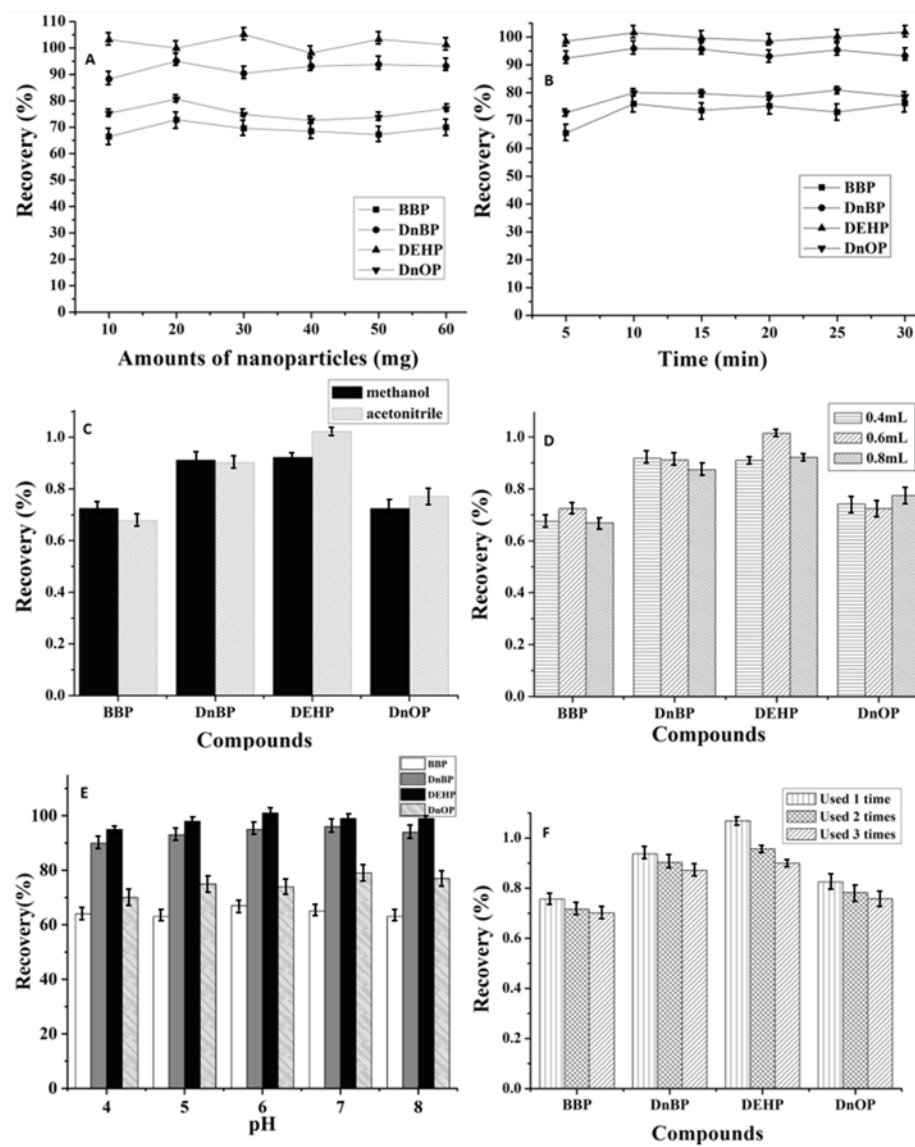


FIG. 5 Optimization of magnetic solid phase extraction conditions: (A) the adsorption amounts, (B) desorption time, (C, D) type and volume of elution solvent, (E) pH, (F) the recyclability of $\text{Fe}_3\text{O}_4@\text{SiO}_2@\text{KCC-1-phenyl}$.

of nanoparticles is needed to achieve an excellent adsorption effect. With the increase in the amount of nanoparticles, the recovery of phthalate acid esters is maintained in an appropriate range. Finally, 20 mg of absorbents was chosen to save the materials and obtain higher recovery in subsequent experiments.

2. Effect of extraction time

To investigate the optimal adsorption conditions, different extraction times (5, 10, 15, 20 and 30 min) were studied. As shown in FIG. 5(B), the extraction efficiency increased as the extraction time increased from 5 min to 10 min, the recoveries of BBP and DnBP were above 75%, and those of DEHP and DnOP were beyond 95%. The recoveries of the phthalate acid esters de-

creased slightly after 10 min. Therefore, the extraction time of 10 min was selected as the optimal extraction time. The absorbents have more efficient active sites after modification by the phenyl groups while still maintaining the original radial-like morphology and structure characteristics. Therefore, the adsorption equilibrium is reached quickly by the radial-like direct channels and larger pores. Meanwhile, the excellent structure is also highly beneficial to the desorption of the targeted compounds.

3. Type and volume of elution solvent

Two solvents, namely, methanol and acetonitrile, were selected to compare their elution efficiency for phthalates. Compared to acetonitrile, methanol does

TABLE I Analytical performance data for the phthalate acid esters by the magnetic solid phase extraction method.

Analytes	Linear range/($\mu\text{g/L}$)	Calibration curve	Correlation coefficient (r^2)	LOD/(ng/L)	RSD*/%
BBP	0.1–20	$y=7090.5x+4760.9$	0.9998	15	3.6
DnBP	0.1–20	$y=6716.1x+6007.1$	0.9993	36	4.1
DEHP	0.1–20	$y=7326.3x+6349.9$	0.9992	48	2.1
DnOP	0.1–20	$y=2457.8x-104.81$	1.0000	58	5.6

* RSD represents relative standard deviation, $n=6$.

not have the effect of π - π interactions and is more hydrophilic, while acetonitrile is a strongly hydrophobic solvent producing a π - π effect with the phthalate ester when it is used as elution agent. The elution efficiencies of the two elution agents are shown in FIG. 5(C). It is observed from the figure that methanol has a better elution effect on BBP and DnBP, and the recovery rate is slightly higher than that using acetonitrile, while acetonitrile has a higher elution efficiency for DEHP and DnOP than methanol, but there is no significant difference between the two solvents. Considering the environmental protection and price, methanol was selected as the eluent.

Changing the amount of methanol used as the eluent, 0.4 mL, 0.6 mL and 0.8 mL of methanol were used to for the elution of the phthalates, and the results are shown in FIG. 5(D). As observed from the figure, the best elution efficiency of BBP, DnBP and DEHP was obtained for 0.6 mL of the methanol eluent. After comprehensive consideration, the dosage of 0.6 mL methanol was selected as the eluent of the method, ensuring that the four phthalates had higher elution efficiency and less methanol.

4. Effect of the pH of the sample solution

In this study, the effect of the sample solution pH was investigated in the range between 4.0 and 8.0 by adjusting the sample solution pH with HCl and NaOH solutions. As can be seen from FIG. 5(E), there was slightly influence on the adsorption efficiency when the water pH was in the range 5.0–8.0. Therefore, there is no need to adjust the sample solution pH in the sample preparation process.

5. Effect of the desorption time

The effect of the elution time on desorption efficiency of the analytes was also investigated. Experiments with different desorption time from 1 min to 20 min were carried out, it was found that all the analytes could be quantitatively desorbed from the sorbent by elution of the sorbent in 10 min.

C. Recyclability of $\text{Fe}_3\text{O}_4@\text{SiO}_2@\text{KCC-1-phenyl}$

To investigate the recyclability of the adsorbent, $\text{Fe}_3\text{O}_4@\text{SiO}_2@\text{KCC-1-phenyl}$ was reused for magnetic solid phase extraction. As shown in FIG. 5(F), the recovery of the targeted compounds was high, and a slightly decrease in the recoveries was observed after reusing. The recoveries of phthalate acid esters were 70.1%, 87.1%, 89.9% and 75.8% for BBP, DBP, and DEHP, and DnOP, respectively, after recycling the nanoparticles four times. The results indicate that $\text{Fe}_3\text{O}_4@\text{SiO}_2@\text{KCC-1-phenyl}$ is relatively stable and reusable.

D. Method validation

The calibration curve characteristics were established by analysing a serial standard solution with different concentrations of phthalate acid esters (Table I). Excellent linearity was obtained with high correlation values ($r^2=0.9992$ – 1.0000) in the range of 0.1–20 $\mu\text{g/L}$. The limits of detection (LOD, $S/N=3$) were calculated to be 15 ng/L for BBP, 36 ng/L for DBP, 48 ng/L for DEHP, and 58 ng/L for DnOP. The results also show excellent method precision with RSDs ranging from 2.1% to 5.6%.

E. Application of the method in real sample

The proposed magnetic solid phase extraction method was further used to analyse the phthalate acid esters of lake water, river water, and tap water samples, combined with HPLC to validate the applicability of the optimized method. As shown in Table II, DEHP and DnOP were detected in river water, and four phthalate acid esters (all except BBP) were detected in lake water. Only DEHP was detected in tap water with the concentrations of 2.16 $\mu\text{g/L}$ which is less than the national standard (8 $\mu\text{g/L}$). To investigate the effect of the sample matrices on the extraction efficiency, the samples were spiked with each target compound at the concentrations of 5 $\mu\text{g/L}$ and 20 $\mu\text{g/L}$. The recoveries of phthalate acid esters in water samples with three repetitions at different concentration levels were 95.8%–100.4% for lake water, 93.0%–103.1% for river

TABLE II The analytical data of the phthalate acid esters (PAEs) in environmental water sample^a.

PAEs	Spiked/($\mu\text{g/L}$)	Lake		River		Tap water	
		Found/($\mu\text{g/L}$)	$R^b/\%$	Found/($\mu\text{g/L}$)	$R^b/\%$	Found/($\mu\text{g/L}$)	$R^b/\%$
DnBP	0	1.48 \pm 0.05		ND ^c		ND	
	0.5	1.96 \pm 0.06	96.2	0.47 \pm 0.03	94.6	0.48 \pm 0.04	96.4
	1.0	2.46 \pm 0.08	98.4	0.98 \pm 0.04	98.2	0.97 \pm 0.05	97.2
BBP	0	ND		ND	-	ND	
	0.5	0.47 \pm 0.05	94.8	0.46 \pm 0.05	93.6	0.49 \pm 0.04	98.2
	1.0	0.97 \pm 0.07	97.2	1.01 \pm 0.08	101.2	0.99 \pm 0.10	99.4
DEHP	0	8.46 \pm 0.18		3.73 \pm 0.06		2.16 \pm 0.08	
	5	13.25 \pm 0.31	95.8	8.74 \pm 0.18	100.2	7.02 \pm 0.12	97.2
	20	28.53 \pm 0.62	100.4	23.9 \pm 0.55	100.9	22.01 \pm 0.49	99.3
DnOP	0	11.81 \pm 0.63		5.01 \pm 0.32		ND	
	5	16.63 \pm 0.87	96.4	9.96 \pm 0.54	98.9	4.94 \pm 0.21	98.8
	20	31.02 \pm 1.75	96.1	25.0 \pm 1.47	99.9	19.65 \pm 1.06	98.3

^a The average of the three measurements.^b R : recovery of the method, $R=(C_{\text{found}}-C_{\text{real}})/C_{\text{added}} \times 100\%$.^c ND: not detected.

TABLE III Comparison of different adsorbents of magnetic solid phase extraction method for the extraction and determination of PAEs from water.

Adsorbent	Linear range/($\mu\text{g/L}$)	LOD/(ng/L)	RSD/%	$R^a/\%$	Reference
magnetic metal-organic framework	0.5–200	80–150	3.1–9.0	85.1–106.7	[10]
Fe@SiO ₂ @PEI	0.5–100	260–450	3.7–4.8	81.5–119	[12]
Magnetic carbon nanotubes	0.2–50	4.9–38	11.7–14.6	65–126	[13]
Fe ₃ O ₄ @ZIF-8	1.0–100	80–240	11.7–14.6	85.6–98.6	[35]
Magnetic PDMS/MWCNTS-OH	0.05–20	10–25		91.5–97.8	[36]
Magnetic graphene	0.1–200	10–56	<8.5	88–110	[37]
Fibrous phenyl functional magnetic mesoporous silica	0.1–20	15–58	2.1–5.6	93–103.4	This work

^a R : recovery of the method.

water, and 97.2%–103.4% for tap water, respectively, demonstrating that the proposed magnetic solid phase extraction method is feasible for sensitive determination of phthalate acid esters in real water samples.

F. Comparison with other reported methods

To evaluate the current method, it was compared with other reported methods for the extraction of phthalate acid esters in terms of the adsorbent material, extraction method, samples, LODs, linearity, recovery and RSD (Table III). The comparison shows that the current method exhibits a comparable or even better LOD, recovery and RSD than the other reported methods. These results further demonstrate that the proposed method is a rapid, sensitive, and repeatable tool for the analysis of trace phthalate acid esters in real samples.

IV. CONCLUSION

The present study demonstrated successful synthesis of fibrous phenyl-functionalized Fe₃O₄@SiO₂@KCC-1 (Fe₃O₄@SiO₂@KCC-1-phenyl) by a facile copolymerization process using PTES as the functional reagent and their application as a new sorbent in magnetic solid phase extraction for extraction and enrichment of phthalate acid esters from the environmental water samples. The obtained Fe₃O₄@SiO₂@KCC-1-phenyl showed monodisperse fibrous spherical morphology, fairly strong magnetic response (29 emu/g), large pore volume (0.44 cm³/g). In addition, Fe₃O₄@SiO₂@KCC-1-phenyl not only can increase adsorption ability of the target analytes, but also improve stability of the NPs and their dispersibility in aqueous media. Under optimum conditions, the Fe₃O₄@SiO₂@KCC-1-phenyl was used for the extraction of four phthalate esters from environmental water samples followed by high-performance liquid chromatographic analysis. Valida-

tion experiments indicated that the developed method presented good linearity (0.1–20 ng/mL), low limit of detection (7.5–29 µg/L, $S/N=3$), and good recoveries (93%–103.4%) in real samples. The comparison with previously reported phthalate acid esters detection methods, owing to the π - π interaction, hydrophobic effect between phthalate acid esters and $\text{Fe}_3\text{O}_4@\text{SiO}_2@\text{KCC-1-phenyl}$, our developed method needs less adsorbent (20 mg) to extract the trace phthalate acid esters from a larger sample volume (500 mL). The amount of organic solvent and time in this work is lower than most of the reported methods.

V. ACKNOWLEDGMENTS

This work was supported by the Commonwealth Scientific Foundation for Industry of Chinese Inspection and Quarantine (No.201210071) of the Ministry of National Science and Technology of China, Chongqing Key Laboratory of Scientific Utilization of Tobacco Resources.

- [1] D. W. Gao and Z. D. Wen, *Sci. Total Environ.* **541**, 986 (2016).
- [2] O. Horn, S. Nalli, D. Cooper, and J. Nicell, *Water Res.* **38**, 3693 (2004).
- [3] M. Vitali, M. Guidotti, G. Macilenti, and C. Cremisini, *Environ. Int.* **23**, 337 (1997).
- [4] B. Tienpont, F. David, E. Dewulf, and P. Sandra, *Chromatographia* **61**, 365 (2005).
- [5] B. Osman, E. T. Ozer, N. Besirli, and S. Gucer, *Polym. Test.* **32**, 810 (2013).
- [6] X. Y. Li, Y. T. Zhang, J. Y. Gui, C. L. Zhang, J. Zhang, and L. Zhang, *Chin. J. Anal. Chem.* **45**, 1375 (2017).
- [7] O. S. Fatoki and A. Noma, *Water Air Soil Poll.* **140**, 85 (2002).
- [8] A. Penalver, E. Pocurull, F. Borrull, and R. M. Marce, *J. Chromatogr. A* **872**, 191 (2000).
- [9] G. Prokupková, K. Holadová, J. Poustka, and J. Hajslova, *Anal. Chim. Acta* **457**, 211 (2002).
- [10] R. Dargahi, H. Ebrahimzadeh, A. A. Asgharinezhad, A. Hashemzadeh, and M. M. Amini, *J. Sep. Sci.* **41**, 948 (2018).
- [11] R. Yang, Y. X. Liu, X. Y. Yan, and S. M. Liu, *Talanta* **161**, 114 (2016).
- [12] Q. X. Zhou, Z. W. Zheng, J. P. Xiao, H. L. Fan, and X. Y. Yan, *Anal. Bioanal. Chem.* **408**, 5211 (2016).
- [13] Y. B. Luo, Q. W. Yu, B. F. Yuan, and Y. Q. Feng, *Talanta* **90**, 123 (2012).
- [14] J. Liu, S. Z. Qiao, Q. H. Hu, and G. Q. Lu, *Small* **7**, 425 (2011).
- [15] D. N. Huang, C. H. Deng, and X. M. Zhang, *Anal. Methods* **6**, 7130 (2014).
- [16] H. Tian, J. Li, Q. Shen, H. L. Wang, Z. P. Hao, L. D. Zou, and Q. Hu, *J. Hazard. Mater.* **171**, 459 (2009).
- [17] A. Stein, *Adv. Mater.* **15**, 763 (2003).
- [18] G. D. Feng, J. Y. Wang, M. Boronat, Y. Li, J. H. Su, J. Huang, Y. H. Ma, and J. H. Yu, *J. Am. Chem. Soc.* **140**, 4770 (2018).
- [19] C. N. Jiao, R. Y. Ma, M. H. Li, L. Hao, C. Wang, Q. H. Wu, and Z. Wang, *Microchim. Acta* **184**, 2551 (2017).
- [20] Q. H. Wu, X. Zhou, M. Sun, X. X. Ma, C. Wang, and Z. Wang, *Microchim. Acta* **182**, 879 (2015).
- [21] M. H. Li, C. N. Jiao, X. M. Yang, C. Wang, Q. H. Wu, and Z. Wang, *J. Sep. Sci.* **40**, 1637 (2017).
- [22] C. Z. Jiang, Y. Sun, X. Yu, L. Zhang, X. M. Sun, Y. Gao, H. Q. Zhang, and D. Q. Song, *Talanta* **89**, 38 (2012).
- [23] M. Behbahani, S. Bagheri, F. Omid, and M. M. Amini, *Microchim. Acta* **185**, 505 (2018).
- [24] H. Shirkhanloo, M. Ghazaghi, A. Rashidi, and A. Vahid, *Microchem. J.* **130**, 137 (2017).
- [25] G. Z. Li, M. Liu, Z. Q. Zhang, C. Geng, Z. B. Wu, and X. Zhao, *J. Colloid. Interf. Sci.* **424**, 124 (2014).
- [26] J. W. Fan, X. M. Wang, W. Teng, J. P. Yang, X. Q. Ran, X. Gou, N. Bai, M. H. Lv, H. W. Xu, G. M. Li, W. X. Zhang, and D. Y. Zhao, *J. Colloid Interf. Sci.* **487**, 354 (2017).
- [27] V. Rebbin, R. Schmidt, and M. Fröba, *Angew. Chem. Int. Edit.* **45**, 5210 (2006).
- [28] Y. Liu, H. Li, and J. M. Lin, *Talanta* **77**, 1037 (2009).
- [29] M. Saraji and N. Khaje, *J. Sep. Sci.* **36**, 1090 (2013).
- [30] Y. Ji, X. Liu, M. Guan, C. D. Zha, H. Y. Huang, H. X. Zhang, and C. M. Wang, *J. Sep. Sci.* **32**, 2139 (2009).
- [31] M. Behbahani, S. Bagheri, F. Omid, and M. M. Amini, *Microchim. Acta* **185**, 11 (2018).
- [32] H. Shirkhanloo, A. Khaligh, H. Z. Mousavi, and A. Rashidi, *Microchem. J.* **124**, 637 (2016).
- [33] X. Zhang, H. Niu, W. Li, L. Y. Shi, and Y. Q. Cai, *Chem. Commun.* **47**, 4454 (2011).
- [34] W. Wang, R. Ma, Q. Wu, C. Wang, and Z. Wang, *Talanta* **109**, 133 (2013).
- [35] R. Hashimoto, Y. Tsuji, and M. Ogawa, *J. Mater. Sci.* **47**, 2195 (2012).
- [36] J. Li, Y. Wei, W. Li, Y. H. Deng, and D. Y. Zhao, *Nanoscale* **4**, 1647 (2012).
- [37] K. J. Yu, X. B. Zhang, H. W. Tong, X. Y. Yan and S. M. Liu, *Mater. Lett.* **106**, 151 (2013).
- [38] X. M. Liu, Z. W. Sun, G. Chen, W. W. Zhang, Y. P. Cai, R. M. Kong, X. Y. Wang, Y. R. Suo, and J. M. You, *J. Chromatogr. A* **1409**, 46 (2015).
- [39] M. Z. Jeddi, R. Ahmadkhaniha, M. Yunesian, and N. Rastkari, *J. Chromatogr. Sci.* **53**, 385 (2015).
- [40] Q. Ye, L. H. Liu, Z. B. Chen, and L. M. Hong, *J. Chromatogr. A* **1329**, 24 (2014).